MATERIALS CHEMISTRY
FRONTIERS

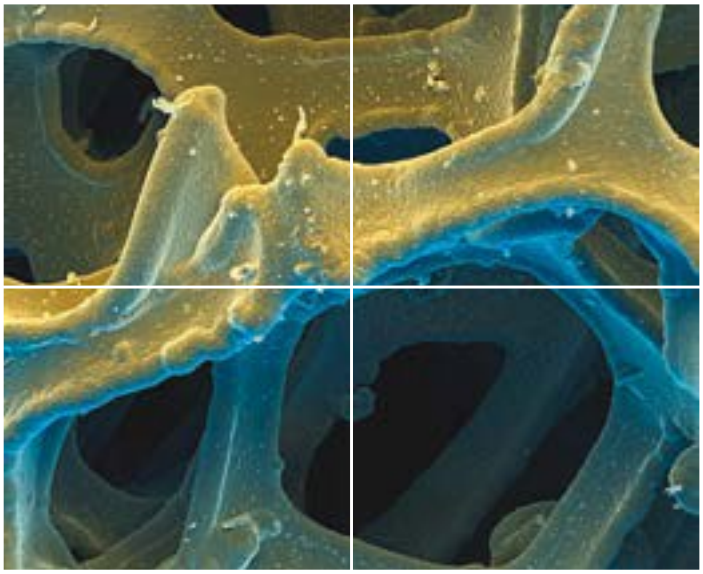

Accepted Manuscript

This article can be cited before page numbers have been issued, to do this please use: I. Sharma, S. R. Dhakate and K. M. Subhedar, *Mater. Chem. Front.*, 2018, DOI: 10.1039/C8QM00082D.

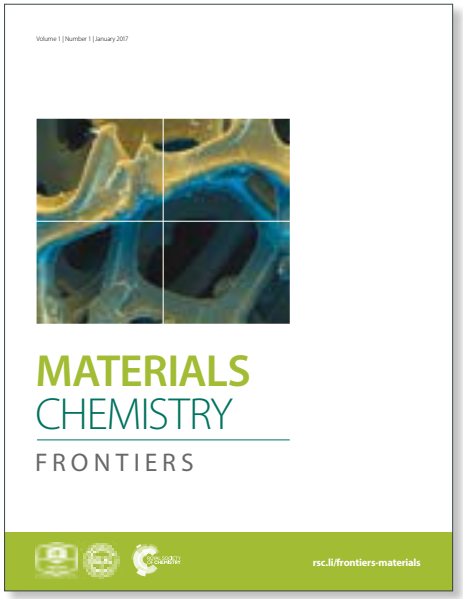

CVD growth of continuous and spatially uniform single layer graphene across grain boundary of preferred (111) oriented copper processed by sequential melting-resolidification-recrystallization

View Article Online
DOI: 10.1039/C8QM00082D

Indu Sharma, Sanjay R. Dhakate and Kiran M. Subhedar*
Advanced Carbon Products, Division of Advanced Materials and Devices,
Academy of Scientific and Innovative Research (AcSIR)-NPL,
CSIR-National Physical Laboratory (NPL), New Delhi-12, India.
**kmsubhedar@gmail.com, kms@nplindia.org*
Tel: +91-11-45721090 (O)

Abstract:

The properties of catalyst used for CVD growth has significant influence on the quality the graphene grown. Single crystalline or preferred (111) oriented with smooth surface is most essential criterion for growth of high quality graphene on copper substrate. Herein, the effective strategy of pre-heat treatment of copper substrate for the growth of improved quality single layer graphene is demonstrated. The sequential melting, resolidification and recrystallization with controlled slow cooling rate leads to preferred (111) oriented grain growth in copper substrate and was confirmed with XRD studies. The grain growth evolution and strain relaxation, correlated with surface smoothening was inferred from AFM studies. The Raman spectroscopy measurement signifies improved quality of the CVD grown graphene which is almost free from multilayer patches that are usually associated with the routine CVD growth process. The Raman mapping carried out directly on graphene/copper surface reveals spatial continuity and uniformity of graphene quality across the copper grain boundaries over large area which signifies the importance of the strain relaxed improved surface morphology with uniform catalytic and crystallographic environment of the beneath surface. The electrical characterization corroborates the result of improved quality of graphene grown on recrystallized copper. Hence, the feasible process of the high quality graphene growth was achieved with simple but effective strategy of preheat treatment involving melting resolidification and recrystallization of copper substrate.

Keywords: Graphene, Chemical vapour deposition (CVD), Crystallization, Raman Spectroscopy

Introduction

Since the discovery single layer graphene with extraordinary properties [1-3], the technological developments in the synthesis of graphene have evolved from trial and hit based micromechanical exfoliation to large scale chemical vapour deposition (CVD) based technique. Amongst these the CVD growth of graphene on copper substrate is most consistent, easily controllable and more important scalable technique[4-7]. However, till now the quality of the CVD grown graphene has not matched with that of micromechanically exfoliated graphene. The electronic and mechanical properties of exfoliated graphene are far better than CVD grown graphene[8-11]. The comparative inferior properties of CVD grown graphene are usually attributed to the presence of crystalline defects and mechanical deformations in the graphene layer[12, 13]. The properties of copper catalyst such as its surface morphology, crystallographic structure and microscopic orientation has pronounced influence on carrier mobility, grain boundaries etc. of the CVD grown graphene. The surface roughness of beneath copper significantly contributes to the quality of graphene[14-16]. The crystallographic orientations of the copper substrate has pivotal role in the CVD growth of graphene. The (111) plane of FCC copper was found to produce best single layer graphene because of several reasons such as it minimizes free energy and maintains hexagonal symmetry with minimum lattice mismatch with graphene [17-20]. Hence, it is very much essential either to use single crystalline or preferred (111) oriented copper substrate for the CVD growth of graphene which are very costly for a scalable CVD process. However, the most widely used cheap and commercially available cold worked copper foils are polycrystalline in nature with poor crystallinity and with very high induced strain. The chemical or electropolishing and annealing can solve the problem of surface roughness and crystallinity only to some extent because polishing can make the mere smoothening of the surface, but it is ineffective in removing the induced strain which is associated with cold rolling process. The annealing process can induce grain growth which is again limited by size of grain and its orientation [21, 22]. The other approaches which have been adopted so far to get desirable and preferred (111) orientation the and CVD growth of high quality graphene includes, the annealing of copper in the presence of hydrogen or to carry out the CVD growth on melted copper substrate which yields high quality sample[23, 24]. However, in the former approach the change of crystallographic orientation of copper to desired (111) orientation, favored by removal surface copper oxide layer with the aid of annealing in the presence of hydrogen. The said recrystallization has been carried out without melting of available copper which might not remove all surface irregularities and there might not be a ultra smooth surface which is required to reduce the nucleation density, an essential condition for growth of high quality graphene and also there could be presence of remnant strain which was induced during manufacturing processing of the foil which may again influence the quality of the CVD grown graphene. In the later approach the CVD growth of single layer graphene on melted copper is no more a self limiting process as the copper evaporates severely at and above its melting point making the Cu surface very unstable and also the generated copper vapors contributes to excess of carbon adatoms which could results in growth of bilayer or multilayer graphene. Hence, the more feasible and suitable approach for high quality graphene growth by CVD should be sequentially to recrystallize the commercially available copper substrate in to preferred oriented (111) substrate by melting and subsequently grow single layer graphene at optimum growth temperature instead of growing it on melted copper.

In light of this, in the present investigations, the single step process for CVD growth of improved quality graphene on preferred (111) orientated smooth and recrystallized copper substrate processed by high temperature heat treatment of commercially available coarsely crystalline copper foil has been demonstrated. Simple and effective approach of sequential melting, resolidification and recrystallization of commercially available copper was employed which produces Cu(111). The XRD and AFM studies were carried out to understand the crystallographic orientation, surface roughness and related strain relaxation of the copper substrate. The quality of the graphene was studied using Raman spectroscopy. The Raman mapping technique was utilized to understand the uniformity and spatial properties of graphene across the copper grain boundaries.

Experimental Section

The growth of graphene was carried on 25 μm thick copper foil (99.8% pure, Alfa Aesar #13382). The foil was thoroughly cleaned with acetone, acetic acid, DI water and IPA. The copper foil was placed inside a quartz reactor at an isothermal zone of a custom built thermal CVD system and evacuated, filled with argon and again pumped down to 0.005 mbar, then heated further under hydrogen flow of 12 sccm at pressure of 0.18 mbar. Prior to graphene growth the copper foil was sequnetialy heat treated for melting, resolidification and recrystallization of copper substrate and finally CVD growth was carried out at 1045°C. In other experiments the foils was also annealed at different tempratures from 980 to 1050°C to study effect of annealing temperature on average grain size. The average grain size was estimated with Average Grain Intercept (AGI) method using optical microscope

image. In this method to quantify the grain or domain size for a given material by drawing a set of randomly positioned line segments on the micrograph, counting the number of times each line segment intersects a grain boundary, and finding the ratio of intercepts to line length. For the growth of graphene at at 1045 °C temperature the methane was introduced with flow rate of 4 sccm for initial time period of 3minutes followed by increase in its flow rate to 25 sccm with total growth time of 30 minutes. After growth the samples were cooled down to 100°C. Methane flow was turned off at 650 °C and hydrogen below 100°C. Finally, the as grown graphene was transfered on Silicon oxide substrate using our established procedures [25]. Optical microscope (Zeiss Axiolab A1) was used to study the grain growth and estimate the size of grains of Copper substrate. X-ray diffraction (XRD) was performed using the Rigaku Diffractometer with CuK_α radiation (λ=1.54Å). Surface morphology was studied using Atomic Force Microscope (AFM, Multimode-V Veeco) and surface roughness was analysed with Research Nanoscope-7.20 software. The micro-Raman mapping was performed under ambient conditions with a Renishaw InVia micro-Raman spectrometer equipped with a 514 nm (2.41eV) wavelength excitation laser and 2400 lines/mm grating. A laser beam size of ~1 μm with ×50 objective lens was used. The electrical contacts pads were deposited on graphene on Si/SiO_2 substrate by thermal evaporation of Au using physical shadow masking technique. The electrical current –voltage chatactristics was measured using two probe method with Kiethely source meter.

Results and discussions

To improve the quality of the graphene growth by CVD, the effect of annealing of copper substrate on its crystallinity was studied. Figure 1 shows surface morphology of the copper substrate as received, preheat treated at 1000 and 1050°C and resolidified and recrystallized sample. These samples are referred as T_0, T_{1000}, T_{1050} and T_{RSC} respectively. The 'as received' sample do not show any visible domains of copper but only show a processing lines resulting from cold rolling process. However, the annealed samples show grain growth of copper. The grain size increases systematically with increase in annealing temperature from 980 to 1060°C. The variation of average grain size as function of inverse temperature is as shown in figure 2. The observed linear relation clearly indicates that the annealing induced grain growth as a consequence of temperature activated diffusion process. The temperature dependent reaction rate is governed by Arrhenius equation,

$$K = Ae^{\frac{-E_a}{k_B T}} \quad \ldots\ldots\ldots\ldots\ldots\ldots\ldots\ldots\ldots\ldots (1)$$

Where, k_B is the Boltzmann constant.

The activation energy according to equation (1) extracted for annealing induced grain growth process was found to be 0.845eV which is considerably lower than corresponding value for bulk copper (1.28eV) [26]. The possible reason for the obtained lower values of activation energy could be the strain originated from grain boundaries. Indeed the cold rolling in foil manufacturing process induces high strain in the foil and in the present case it is found that even high temperature annealing could not to reduce the strain in foil significantly.

To investigate further, prior to growth of graphene the Cu substrate was heated to 1080°C which is very close to its melting point (1084.6°C). At this temperature the copper is in semi-molten state but not in complete liquid state. Further small increase in the temperature leads to complete melting of copper and its ball formation takes place because of its dewetting with supporting quartz plate on which the foil is rested during heat treatment. The copper foil was kept there at 1080°C for 10 min and then cooled down to 1000°C for its resolidification and recrystallization. The X-ray diffraction (XRD) was carried out for samples with different heat treatment processes. Figure 3 shows XRD pattern of as-received (T_0) copper foil, annealed samples T_{1000}, T_{1050} and the resolidified and recrystallized sample (T_{RSC}). The T_0 and other annealed sample shows (002) dominated peak along with small intensity (111) and (220) peaks. However, the T_{RSC} sample shows only (111) peak implying that the melting and subsequent resolidification of copper substrate leads to recrystallization of copper foil. The XRD patterns of recrystallized copper consistently show a single peak of (111) with complete suppression of peaks of other planes which are otherwise present before recrystallization. In order to confirm spatial variations of the crystallographic structure the same sample was measured few times such that the data will be collected from different areas of the sample. The results of these measurements on the same sample and also in different samples recrystallized with similar pre-treatment condition show consistent result and confirming the formation preferred oriented copper (111). It is noteworthy to mention that the solidification was carried out with slow cooling (with rate less than 3°C per minute) which could have resulted in the complete recrystallization of copper. Interestingly the recrystallization comes up with preferred (111) oriented domains. The Cu generally crystallizes in the simple FCC crystal structure, where the low indices (100), (110), and (111) surfaces are with the lowest surface energy. Further Robinson et al. [27] has reported that Cu(111) orientation is with lower surface energy among the lower index crystalline surface. Secondly, the dewetting of copper in molten state during heat treatment is very crucial as the weaker interaction of

the foil with supporting quartz plate lead to minimization of interfacial energy. Usually for the grain growth there exist grain orientation specific driving forces. The top and bottom surface of the foil are associated with the excess free energy γ_s. The bottom surface will have additional excess free energy γ_i arising from its interface with supporting quartz plate. Both γ_s (the energy of the free surface) and γ_i, depend strongly on the orientation of a grain with respect to the plane of the foil. Typically, for FCC metals on amorphous substrates like quartz or fused silica, both γ_s and γ_i are minimized for grains with (111) texture. Implying that growth of grains with (111) texture is generally preferred over growth of grains with other orientations [28]. This can result in the development of bimodal grain size distributions [29], in which the large grains have γ_s and γ_i minimizing orientations. Further large grains consume all other grains, resulting in a population of grains with a monomodal size distribution which here is preferred (111) orientation of copper grains with respect to the plane of the foil. This recrystallization of copper with preferred (111) orientation is very crucial for further growth of graphene by CVD technique.

The induced strain in the materials has pronounced effect on its surface morphology and signatures of the strain relaxation can be easily seen from surface roughness variations. Figure 4 shows atomic force microscope (AFM) images of as-received (T_0) copper foil, annealed samples T-1000, T-1050 and resolidified and recrystallized sample (T_{RSC}). The morphology of 'As received' sample shows grooves on the surface which was also observed from optical images as. The T-1000 and T-1050 sample shows improvement in surface morphology with decreasing surface roughness. The AFM image of T_{RSC} shows very flat and smooth surface as a consequence of melting and resolidification of the copper foil. The average surface roughness (Ra) and root mean square surface roughness (Rq) estimated for T_0, T-1000, T-1050 and T_{RSC} are tabulated in table 1. The surface roughness values found to decrease more drastically for resolidified and recrystallized sample (Ra from 56.7 to 1.4 nm) compared to other annealed samples indicating significant relaxation of the induced strain in the foil. The observed correlation of surface roughness with induced strain is consistent with earlier studies [30, 31]. The employed sequence of resolidification and recrystallization of copper substrate leads to strain relaxed with smooth surface and preferred (111) orientated grain growth. Here getting the strain relaxed smooth surface of the resolidified and recrystallized copper substrate is the other critical and important aspect which further contributes for better quality of CVD grown single layer graphene because the smooth surface with reduced edges and enhanced terraces reduces the nucleation density and leads to the growth of graphene with less grain boundary effects[32-34].

Sample	Ra (nm)	Rq (nm)
T_0	56.7	69.4
T-1000	39.9	47.6
T-1050	11.2	14.8
T_{RSC}	1.44	3.17

Table1. Aaverage surface roughness (Ra) and root mean square surface roughness (Rq) for T_0, T-1000, T-1050 and T_{RSC}.

The precondition of the copper substrate like its grain size and crystallographic orientations, crystallinity, and surface morphology has pronounced effects on the properties of CVD grown graphene. The Cu(111) plane produces graphene with superior quality, with less defect and minimal coverage of multilayer patches and having high coverage of single layer [17, 19]. Hence, the resolidification and recrystallization process which results in Cu(111) oriented strain relaxed with smooth surface is very much crucial for the growth of high quality graphene on commercial available copper foil and hence the process was further used to preheat treat the Cu substrate prior to the CVD growth of graphene.

The CVD growth of graphene is reported in wide window of temperature range from 850 to 1090°C. Though the higher growth temperature produces better graphene, the CVD growth process at very high temperature leads to higher fraction of multilayer region because at high temperature around its melting point the evaporation rate of Cu is very high even at high or atmospheric pressure CVD growth process and the catalytic activity of resulted copper in vapor phase contributes to multilayer graphene. In our low pressure CVD growth process, we tried to grow the graphene on melted copper at 1080°C which leads to growth of discontinuous graphene layer or patches which are again with multilayer nature because of the catalytic activity of copper vapors and extremely unstable copper surface as a result of sever evaporation of copper atoms at this high temperature and low growth

View Article Online
DOI: 10.1039/C8QM00082D

pressure. Hence, prior to growth of graphene and after melting at 1080°C, the Cu substrate was slowly cooled down to 1000°C (T_S) and stabilized at this temperature for ten minutes and again raised to its growth temperature, T_G of 1045°C and CVD growth was carried out. The melting followed by slow cooling resulting recrystallization is very much crucial for getting uniform single layer graphene of high quality. The employed growth scheme is as shown in figure 5. Here, in addition to preferred orientation of Cu substrate and its surface improvement, the sequence of melting, resolidification and recrystallization is also very much important for the actual CVD process for high quality graphene growth. There are other reported methods[35, 36] to produce monocrystalline Cu(111) in which the Cu foil is either annealed for long time for about 12 hours at annealing temperature or the starting Cu foil is chemically polished and then annealed at temperature below its melting and the process is repeated several times so as to get single (111) domain. This makes the whole process as a time and energy consuming. Further, the process can be prone to contamination because of involved chemical treatment or long duration of the process. In contrast the present work demonstrates a fast process which produces copper domain with preferred orientation of (111) although with limited size. However, interestingly during CVD growth on this preferred oriented copper substrate, the single layer graphene grow without any impediment across the domain boundary of preferred oriented Cu (111). The spatial uniformity of graphene quality across the Cu(111) domain was then further confirmed with Raman mapping.

Different characterization techniques are being used to judge the quality of the graphene. The Raman spectroscopy is being the best and most commonly used technique to decide the ultimate quality of the graphene on the basis of induced defects, number of layers, doping of impurities and even incorporated strain etc. In Raman spectroscopy the quality of the graphene is judged from evaluation of different parameters such as peak position, peak width (FWHM) and relative ratios of the intensity for the G, 2D and D peaks [37, 38]. The stress in the sample can lead to red or blue shift in position of 2D peak depending upon nature strain like compressive or tensile. The charge carrier doping also show similar effects. The intensity ratios I_D/I_G and I_{2D}/I_G are the measures used for determining the quality of single layer of graphene. The Raman mapping of these quantities give the spatial uniformity of the graphene quality. Figure 6 shows (a) Raman spectra of CVD grown single layer graphene on Si/SiO_2 substrate with prior process of resolidification and recrystallization (Inset of the figure shows its image) and its corresponding Raman mapping images for peak intensity ratios (b) I_D/I_G and (c) I_{2D}/I_G, (d) 2D peak FWHM (cm^{-1}) and (e) 2D peak position (cm^{-1}). The I_{2D}/I_G and I_D/I_G ratios derived from D, G and 2D peak mapping are around 3.2 and 0.1 respectively indicating superior quality of the CVD grown graphene. The average of I_{2D}/I_G and I_D/I_G ratios taken for number of sample are about 3 and 0.1 respectively showing reproducibility of the process. Further, the 2D peak has FWHM is about $29cm^{-1}$ usually about same for exfoliated graphene indicating high quality of the CVD grown single layer graphene. The position of the 2D is at $2685cm^{-1}$ and without any energy shift in Raman shift again indicating the graphene without doping or induced strain. The variation of colour contrast in the optical micrograph of the graphene transferred onto the Si/SiO_2 wafer can be used to distinguish the single layer and multilayer graphene easily [39] and the concept is used to estimate the percentage of the single layer coverage over large area and which in the case recrystallized sample is about 98%.

Further, to understand the quality of graphene with respect to copper grains on which it is grown and its uniformity across the grain boundaries, Raman mapping was carried out directly on graphene/copper surface to reveal the spatial continuity and uniformity of graphene properties across the copper grain boundary. The I_D/I_G and I_{2D}/I_G ratios are used for determining the quality graphene which in turn influenced by properties of copper surface such as its roughness and its crystallographic orientations. Hence, the difference in grain orientation or difference in their nature and density of defects and smoothness is expected to get reflected in the measured properties of graphene across the grain boundaries of copper. Moreover, the grain boundary associated with such graphene gives significant D peak intensity [13]. Hence, the presence of graphene grain boundary is expected to show its signatures in the Raman mapping. Figure 7 shows (a) Optical image of graphene on copper across grain boundary area in which Raman mapping (red shaded area) was carried out and its (b) Raman spectra. The mapping of intensity ratios (c) I_D/I_G and (d) I_{2D}/I_G derived from Raman mapping of G, 2D and D peaks for CVD graphene grown on resolidified and recrystallized copper substrate across the grain boundary. The mapping of I_D/I_G and I_{2D}/I_G ratios do not show any abrupt variation or discontinuity across the copper grain boundary implying that the beneath copper surface of different grains providing consistent environment for the CVD growth of the continuous and uniform single layer graphene without grain boundary across the copper grain boundary. This indicates that the neighboring grains are having uniform crystallographic properties in terms of their surface roughness and related strain, catalytic properties and defects which are mainly controlled by crystallographic orientations. This evidentially confirms the growth of high quality uniform single layer graphene which was supported by the XRD and AFM

results again confirming strain relaxed, smooth preferred orientation of (111) copper grains by resolidification and recrystallization copper substrate.

View Article Online
DOI: 10.1039/C8QM00082D

Finally, the electrical measurements on CVD graphene grown on resolidified and recrystallized copper substrate were carried out. Figure 8 shows plot for Current-voltage (I-V) characteristics of CVD grown graphene transferred on Si/SiO_2(300nm) substrate. The measured current-voltage (I-V) characteristics using two-probe method gives graphene resistance value of 1.6kΩ. This observed value of resistance is consistent with values reported in the literature[40, 41]. Moreover, the measured value in the present investigation was obtained from two probe measurement method which also includes the contact resistance of the electrical contacts to graphene in addition to the graphene resistance. Hence, the actual resistance of the graphene should be less than the measured value of 1.6kΩ. An empirical relation between carrier mobility (μ) and full width at half maxima (FWHM) of the 2D peak (Γ_{2D}) has been developed based on measured data of carrier mobility and different parameters in Raman spectroscopy for five types of CVD graphene prepared using different catalysts, feed gases, and CVD methods[42]. Based on this analysis they found that the FWHM of the 2D peak was closely related to the carrier mobility regardless the type of graphene. In particular, the logarithmic value of the mobility due to long-range scattering show linear relationship with the FWHM of the 2D peak as follows,

$$\log \mu = \alpha + \beta.\Gamma_{2D} \quad \ldots\ldots\ldots\ldots\ldots\ldots\ldots\ldots(2)$$

With α and β constants obtained from the fitting of line given by equation (2) using different measured data having values of 12.157 and −0.116 respectively. With these constant the final empirical relation between carrier mobility (μ) and FWHM of the 2D peak (Γ_{2D}) obtained as

$$\log \mu = 12.157\text{-}0.116 \,.\, \Gamma_{2D} \quad \ldots\ldots\ldots\ldots\ldots\ldots\ldots(3)$$

The measurements carried out on graphene sample prepared by mechanically exfoliation and epitaxial graphene grown on SiC also fits well with this empirical relation.

In the present investigation the estimated carrier mobility (μ) of the CVD graphene grown on recrystallized copper substrate using equation (3) found out to be 6580cm^2/V.s for the measured 2D peak FWHM (Γ_{2D}) of about 29 cm^{-1} for graphene on SiO_2 substrate. This estimated value of carrier mobility is reasonably superior compared to other reported CVD grown graphene samples. Moreover, the obtained carrier mobility is comparable to the mechanically exfoliated sample which generally supposed to be are of the best quality. This proves the worth of the very much essential process of melting-resolidification-recrystallization of copper substrate for producing high quality graphene by CVD technique.

Conclusions

The effective strategy of preheat treatment of copper substrate for the growth of improved quality single layer graphene is demonstrated. The sequential melting, resolidification and recrystallization with controlled cooling rate leads to preferred (111) oriented grain growth in copper substrate and was confirmed with XRD studies. The possible reason for preferred (111) oriented grain growth in copper is the low surface energy of lower index of (111) plane and minimization of interfacial energy resulting from weak interaction of FCC copper surface with the quartz substrate.The grain growth evolution and strain relaxation with surface smoothening was inferred from AFM studies. The Raman spectroscopy measurement signifies improved quality of the CVD grown graphene which is almost free from multilayer patches that are associated with the usual CVD growth process. The Raman mapping carried out directly on graphene/copper surface reveals spatial continuity and uniformity of graphene quality across the copper grain boundaries confirmed the results of surface improvement with uniform catalytic and crystallographic environment of the beneath surface. It signifies the importance of the employed pre-treatment of melting resolidification and recrystallization process which leads to single step and feasible CVD process of the high quality continuous graphene growth with simple but effective strategy. The electrical characterization and estimated high carrier mobility corroborates the high quality of the CVD grown graphene on recrystallized copper substrate. The present study will advance the understanding about the relevance of structure and surface properties of copper substrate with the quality of the graphene grown and will help to establish a better CVD process for growth of improved quality single layer graphene which is still a challenging task.

Acknowledgments

Authors are thankful to CSIR for supporting this work. Authors are thankful to Sandip singh for his help in AFM measurements.

Conflict of interest: There are no conflicts to declare.

View Article Online
DOI: 10.1039/C8QM00082D

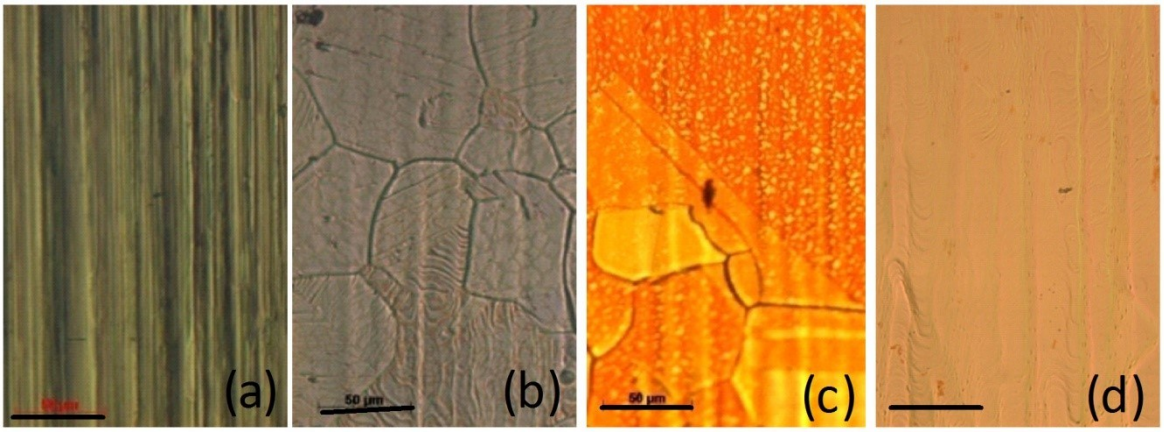

Fig.1 Optical images of (a) as-received copper foil (T_0), annealed samples at (b) 1000°C(T_{1000}), (c)1050°C(T_{1050}) and (d) resolidified and recrystallized sample (T_{RSC}) (scale bar-50µm)

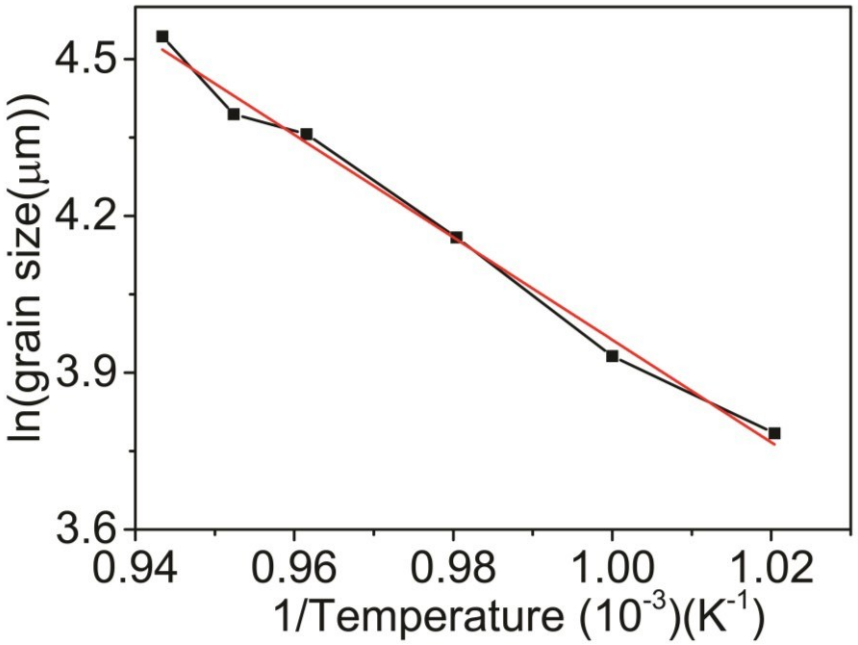

Fig.2 Arrhenius plot for variation of average grain size as a function of inverse temperature

View Article Online
DOI: 10.1039/C8QM00082D

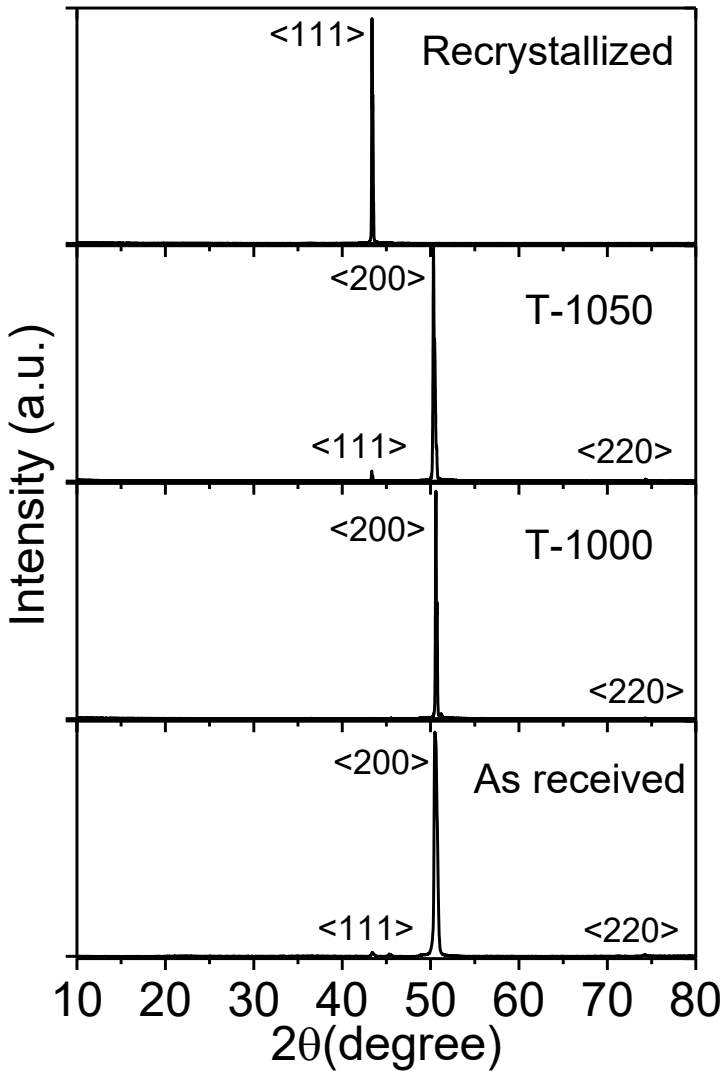

Fig.3 XRD pattern of as-received (T_0) copper foil, annealed samples T-1000, T-1050 and resolidified and recrystallized sample (T_{RSC})

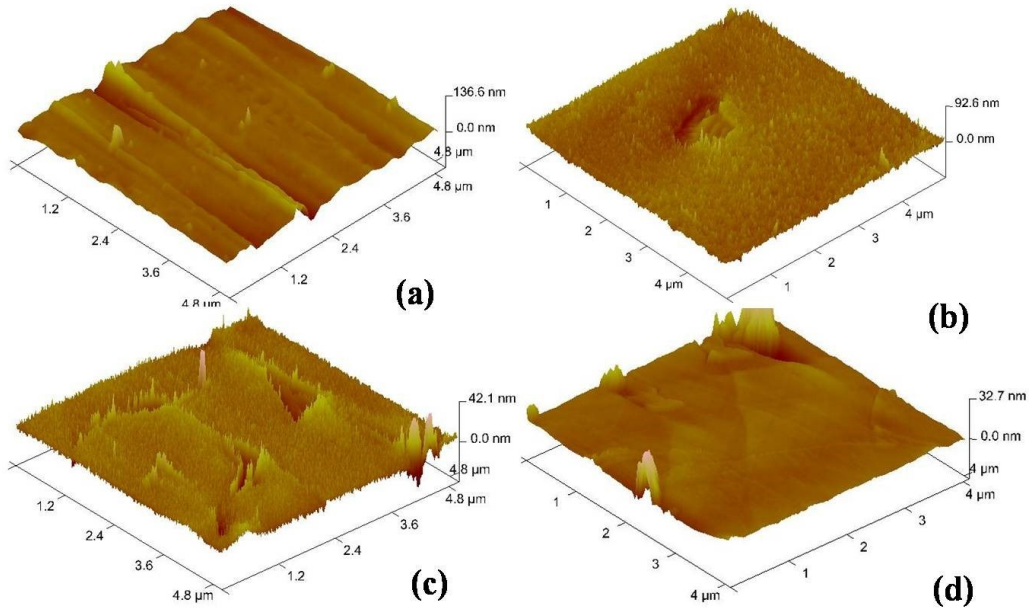

Fig. 4 Atomic force microscope (AFM) images of (a) as-received (T_0) copper foil, (b) annealed sample T-1000, (c) T-1050 and (d) resolidified and recrystallized sample (T_{RSC})

View Article Online
DOI: 10.1039/C8QM00082D

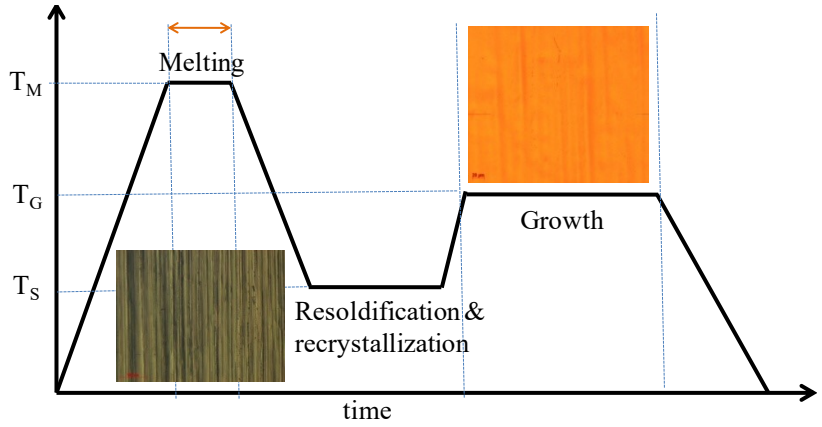

Fig.5 Schematic of step wise process employed for CVD growth of graphene with melting, resolidification and recrystallization

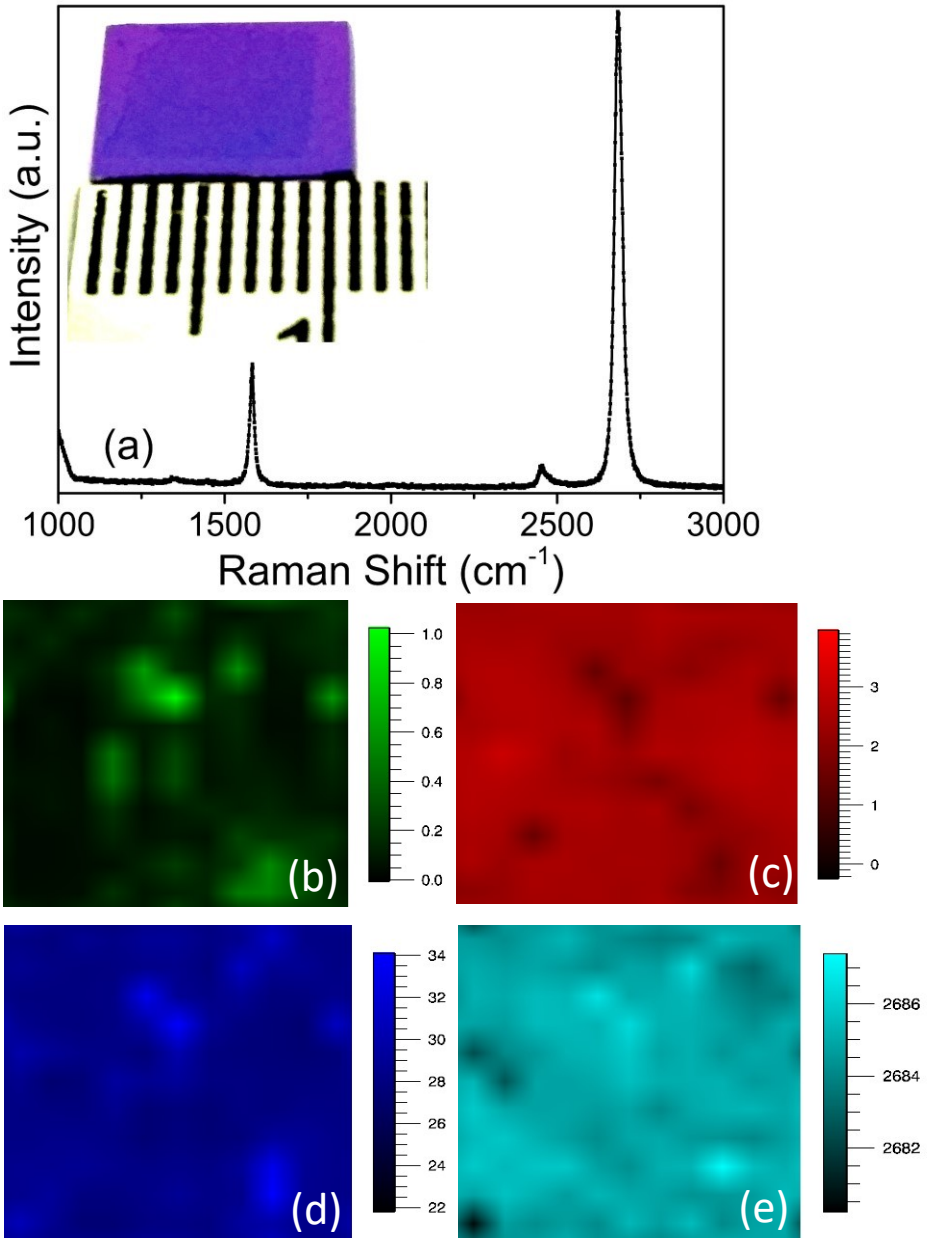

Fig.6 (a) Raman spectra of CVD grown single layer graphene on Si/SiO_2 substrate with prior process of resolidification and recrystallization (Inset its Photograph) and its corresponding Raman mapping images for peak intensity ratios (b) I_D/I_G and (c) I_{2D}/I_G, (d) 2D peak FWHM (cm^{-1}) and (e) 2D peak position (cm^{-1}) (The area selected for mapping is 10 by10 μm)

View Article Online
DOI: 10.1039/C8QM00082D

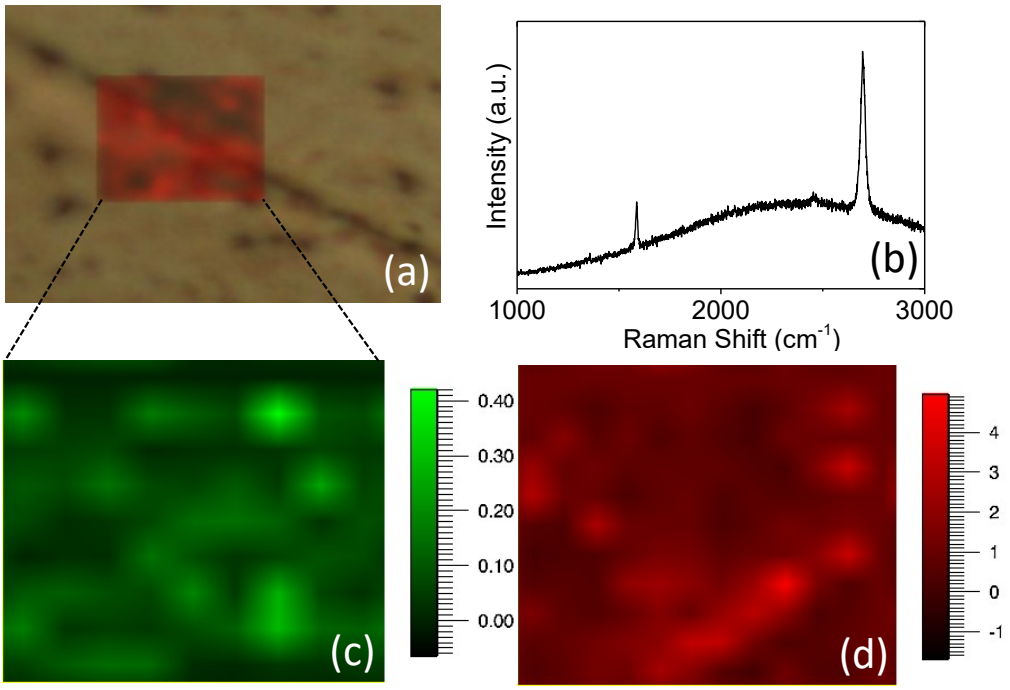

Fig.7 (a) Optical image of graphene on copper across grain boundary area which is selected for Raman mapping (red shaded area) and its (b) Raman spectra. The intensity ratios (c) I_D/I_G and (d) I_{2D}/I_G derived from Raman mapping of G, 2D and D peaks for CVD graphene grown on resolidified and recrystallized copper substrate across the grain boundary. (The area selected for mapping is 10 by12 μm)

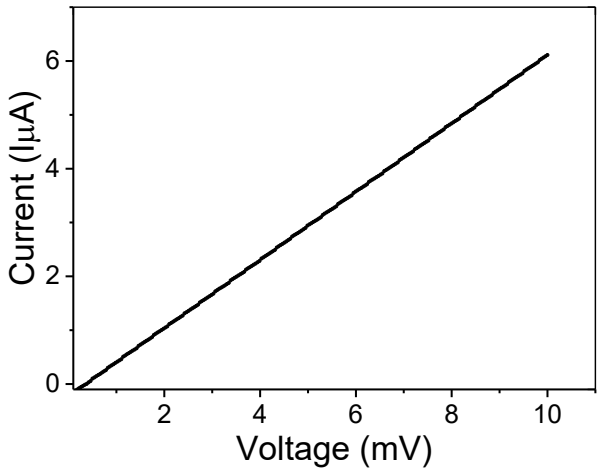

Fig.8 Current-voltage (I-V) characteristics of CVD graphene grown on resolidified and recrystallized copper substrate.

References

1. K. S. Novoselov, A. K. Geim, S. V. Morozov, D. Jiang, Y. Zhang, S. V. Dubonos, I. V. Grigorieva and A. A. Firsov, *Science*, 2004, **306**, 666-669.
2. K. S. Novoselov, A. K. Geim, S. Morozov, D. Jiang, M. Katsnelson, I. Grigorieva, S. Dubonos, Firsov and AA, *Nature*, 2005, **438**, 197-200.
3. A. K. Geim and K. S. Novoselov, *Nat Mater*, 2007, **6**, 183-191.
4. X. Li, W. Cai, J. An, S. Kim, J. Nah, D. Yang, R. Piner, A. Velamakanni, I. Jung, E. Tutuc, S. K. Banerjee, L. Colombo and R. S. Ruoff, *Science*, 2009, **324**, 1312-1314.
5. X. Li, C. W. Magnuson, A. Venugopal, R. M. Tromp, J. B. Hannon, E. M. Vogel, L. Colombo and R. S. Ruoff, *Journal of the American Chemical Society*, 2011, **133**, 2816-2819.

6. S. Bae, H. Kim, Y. Lee, X. Xu, J.-S. Park, Y. Zheng, J. Balakrishnan, T. Lei, H. R. Kim and Y. I. Song, *Nat Nanotechnol*, 2010, **5**, 574-578.
7. Z. Yan, J. Lin, Z. Peng, Z. Sun, Y. Zhu, L. Li, C. Xiang, E. L. Samuel, C. Kittrell and J. M. Tour, *Acs Nano*, 2012, **6**, 9110-9117.
8. K. S. Novoselov, V. Fal, L. Colombo, P. Gellert, M. Schwab and K. Kim, *Nature*, 2012, **490**, 192-200.
9. S. Morozov, K. Novoselov, M. Katsnelson, F. Schedin, D. Elias, J. A. Jaszczak and A. Geim, *Phys Rev Lett*, 2008, **100**, 016602.
10. N. Cernetic, S. Wu, J. A. Davies, B. W. Krueger, D. O. Hutchins, X. Xu, H. Ma and A. K. Y. Jen, *Adv Funct Mater*, 2014, **24**, 3464-3470.
11. X. Zhang, A. Hsu, H. Wang, Y. Song, J. Kong, M. S. Dresselhaus and T. s. Palacios, *Acs Nano*, 2013, **7**, 7262-7270.
12. P. Y. Huang, C. S. Ruiz-Vargas, A. M. van der Zande, W. S. Whitney, M. P. Levendorf, J. W. Kevek, S. Garg, J. S. Alden, C. J. Hustedt and Y. Zhu, *Nature*, 2011, **469**, 389-392.
13. Q. Yu, L. A. Jauregui, W. Wu, R. Colby, J. Tian, Z. Su, H. Cao, Z. Liu, D. Pandey and D. Wei, *Nat Mater*, 2011, **10**, 443-449.
14. Z. Luo, Y. Lu, D. W. Singer, M. E. Berck, L. A. Somers, B. R. Goldsmith and A. C. Johnson, *Chemistry of Materials*, 2011, **23**, 1441-1447.
15. D. Lee, G. D. Kwon, J. H. Kim, E. Moyen, Y. H. Lee, S. Baik and D. Pribat, *Nanoscale*, 2014, **6**, 12943-12951.
16. G. D. Kwon, E. Moyen, Y. J. Lee, Y. W. Kim, S. H. Baik and D. Pribat, *Materials Research Express*, 2017, **4**, 015604.
17. J. D. Wood, S. W. Schmucker, A. S. Lyons, E. Pop and J. W. Lyding, *Nano Lett*, 2011, **11**, 4547-4554.
18. A. T. Murdock, A. Koos, T. B. Britton, L. Houben, T. Batten, T. Zhang, A. J. Wilkinson, R. E. Dunin-Borkowski, C. E. Lekka and N. Grobert, *Acs Nano*, 2013, **7**, 1351-1359.
19. L. Zhao, K. T. Rim, H. Zhou, R. He, T. F. Heinz, A. Pinczuk, G. W. Flynn and A. N. Pasupathy, *Solid State Communications*, 2011, **151**, 509-513.
20. L. Tao, J. Lee, H. Chou, M. Holt, R. S. Ruoff and D. Akinwande, *Acs Nano*, 2012, **6**, 2319-2325.
21. M. D. S. L. Wimalananda, J.-K. Kim and J.-M. Lee, *Carbon*, 2016, **108**, 127-134.
22. K. P. Sharma, S. M. Shinde, M. S. Rosmi, S. Sharma, G. Kalita and M. Tanemura, *Journal of materials science*, 2016, **51**, 7220-7228.
23. Y. A. Wu, Y. Fan, S. Speller, G. L. Creeth, J. T. Sadowski, K. He, A. W. Robertson, C. S. Allen and J. H. Warner, *Acs Nano*, 2012, **6**, 5010-5017.
24. J. Hu, J. Xu, Y. Zhao, L. Shi, Q. Li, F. Liu, Z. Ullah, W. Li, Y. Guo and L. Liu, *Sci Rep-Uk*, 2017, **7**, 45358.
25. K. M. Subhedar, I. Sharma and S. R. Dhakate, *Phys Chem Chem Phys*, 2015, **17**, 22304-22310.
26. S. Ganapathi, D. Owen and A. Chokshi, *Scripta metallurgica et materialia*, 1991, **25**, 2699-2704.
27. Z. R. Robinson, P. Tyagi, T. M. Murray, C. A. Ventrice Jr, S. Chen, A. Munson, C. W. Magnuson and R. S. Ruoff, *Journal of Vacuum Science & Technology A: Vacuum, Surfaces, and Films*, 2012, **30**, 011401.
28. C. V. Thompson and R. Carel, *Journal of the Mechanics and Physics of Solids*, 1996, **44**, 657-673.
29. H. Frost, C. Thompson and D. Walton, *Acta metallurgica et materialia*, 1992, **40**, 779-793.
30. A. Perron, O. Politano and V. Vignal, *Surface and Interface Analysis*, 2008, **40**, 518-521.
31. M. R. Stoudt and R. E. Ricker, *Metallurgical and Materials Transactions A*, 2002, **33**, 2883-2889.
32. Q. Yuan, B. I. Yakobson and F. Ding, *The journal of physical chemistry letters*, 2014, **5**, 3093-3099.
33. J. Gao, J. Yip, J. Zhao, B. I. Yakobson and F. Ding, *Journal of the American Chemical Society*, 2011, **133**, 5009-5015.
34. S. Wang, H. Hibino, S. Suzuki and H. Yamamoto, *Chemistry of Materials*, 2016, **28**, 4893-4900.
35. V. L. Nguyen, B. G. Shin, D. L. Duong, S. T. Kim, D. Perello, Y. J. Lim, Q. H. Yuan, F. Ding, H. Y. Jeong, H. S. Shin, S. M. Lee, S. H. Chae, Q. A. Vu, S. H. Lee and Y. H. Lee, *Adv Mater*, 2015, **27**, 1376-1382.

36. L. Brown, E. B. Lochocki, J. Avila, C.-J. Kim, Y. Ogawa, R. W. Havener, D.-K. Kim, E. J. Monkman, D. E. Shai, H. I. Wei, M. P. Levendorf, M. Asensio, K. M. Shen and J. Park, *Nano Lett*, 2014, **14**, 5706-5711.
37. A. C. Ferrari, J. Meyer, V. Scardaci, C. Casiraghi, M. Lazzeri, F. Mauri, S. Piscanec, D. Jiang, K. Novoselov and S. Roth, *Phys Rev Lett*, 2006, **97**, 187401.
38. A. C. Ferrari and D. M. Basko, *Nat Nanotechnol*, 2013, **8**, 235-246.
39. P. Blake, E. Hill, A. Castro Neto, K. Novoselov, D. Jiang, R. Yang, T. Booth and A. Geim, *Appl Phys Lett*, 2007, **91**, 063124.
40. I. Kazuyuki, K. Masayuki, S. Tadashi and A. Yuji, *Japanese Journal of Applied Physics*, 2013, **52**, 06GD08.
41. S. Kumar, A. Kumar, A. Tripathi, C. Tyagi and D. K. Avasthi, *J Appl Phys*, 2017, **123**, 161533.
42. Y. S. Woo, D. W. Lee and U. J. Kim, *Carbon*, 2018, **132**, 263-270.